

A. Salmi, T. Tala, C. Bourdelle, P. Mantica, L. Meneses, S. Mordjick,
H. Bufferand, M. Clever, J. Svensson, P. Tamain, M. Groth, J. Hillesheim,
C. Maggi, M. Maslov, V. Naulin, J. Juul Rasmussen, G. Sips,
A. Sirinelli, M. Tsalas, H. Weisen, M. Wischmeier
and JET EFDA contributors

Gas Puff Modulation Experiments in JET L- and H-Mode Plasmas

“This document is intended for publication in the open literature. It is made available on the understanding that it may not be further circulated and extracts or references may not be published prior to publication of the original when applicable, or without the consent of the Publications Officer, EFDA, Culham Science Centre, Abingdon, Oxon, OX14 3DB, UK.”

“Enquiries about Copyright and reproduction should be addressed to the Publications Officer, EFDA, Culham Science Centre, Abingdon, Oxon, OX14 3DB, UK.”

The contents of this preprint and all other JET EFDA Preprints and Conference Papers are available to view online free at www.iop.org/Jet. This site has full search facilities and e-mail alert options. The diagrams contained within the PDFs on this site are hyperlinked from the year 1996 onwards.

Gas Puff Modulation Experiments in JET L- and H-Mode Plasmas

A. Salmi¹, T. Tala¹, C. Bourdelle², P. Mantica³, L. Meneses⁴, S. Mordjick⁵,
H. Bufferand², M. Clever⁶, J. Svensson⁷, P. Tamain², M. Groth⁸, J. Hillesheim⁹,
C. Maggi¹⁰, M. Maslov⁹, V. Naulin¹¹, J. Juul Rasmussen¹¹, G. Sips¹²,
A. Sirinelli¹³, M. Tsalas¹⁴, H. Weisen¹⁵, M. Wischmeier¹⁰
and JET EFDA contributors*

JET-EFDA, Culham Science Centre, OX14 3DB, Abingdon, UK

¹VTT, Espoo, Finland;

²IRFM-CEA, Saint Paul lez Durance, France;

³IFP, CNR-ENEA, Milan, Italy;

⁴IST, Lisbon, Portugal;

⁵College of William & Mary, Virginia, USA;

⁶FZJ, Jülich, Germany,

⁷IPP, Greifswald, Germany,

⁸Aalto University, Helsinki, Finland;

⁹CCFE, Abingdon, UK;

¹⁰IPP, Garching, Germany;

¹¹DTU Physics, Lyngby, Denmark;

¹²EFDA CSU, Culham,

¹³ITER, France,

¹⁴DIFFER, Nieuwegein, Netherlands;

¹⁵CRPP, Lausanne, Switzerland.

* See annex of F. Romanelli et al, "Overview of JET Results",
(24th IAEA Fusion Energy Conference, San Diego, USA (2012)).

Preprint of Paper to be submitted for publication in Proceedings of the
41st EPS Conference on Plasma Physics, Berlin, Germany
23rd June 2014 – 27th June 2014

INTRODUCTION

JET experiments utilising gas puff modulation technique [1-5] have been carried out in both L- and H-mode plasmas to study plasma fuelling through the pedestal as well as particle sources and transport. The H-mode experiment is the first exploration of this technique on JET H-mode conditions and focuses on verifying the potential of this technique. The modulation technique, equations and the H-mode experiment (ITER like wall) are described first while the L-mode collisionality scan results (Carbon wall) are given at the end.

1. EXPERIMENTAL SETUP

The H-mode discharges are run in the corner configuration with low triangularity, $B_t = 2.7T$, $I_p = 2.0MA$, $n_{e0} = 6 \times 10^{19}m^{-3}$, $T_{e0} = 3.5keV$. Figure 1 illustrates the various gas injection locations used in these discharges on poloidal plane. The top and midplane GIMs can be considered as point sources while the ones at the divertor are nearly axisymmetric. GIM 12 was on in all discharges with constant gas rate of $\sim 1.5e22$ 1/s while the others were modulated (one at a time) using 2–4Hz rectangular waveform with 50% duty cycle going from 0 to $\sim 1.5e22$ 1/s. The small equilibrium modulation due to the gas is removed by mapping the data on flux coordinates before calculating the amplitude and phase profiles. The plasma response (electron density modulation) is measured with a multi-band reflectometer (KG10) capable of good spatial and temporal resolution [6]. This data was found to agree well with the Thomson Scattering both in steady state and in temporal response.

2. ELECTRON DENSITY EVOLUTION

In interpreting the measurements we assume that the electron density evolution follows the usual 1.5D equation for non-cylindrical and axisymmetric plasmas and that the transport does not evolve in time

$$\frac{\partial}{\partial t}(V'n_e) = \frac{\partial}{\partial \rho} \left[V' \langle (\nabla \rho)^2 \rangle \left(D \frac{\partial n_e}{\partial \rho} - v n_e \right) \right] + V'S. \quad (1)$$

Here ρ is the normalised square root of toroidal flux, $V'(\rho)$ is the radial derivative of the plasma volume, $D(\rho)$ and $v(\rho)$ are the diffusion and convection profiles, $S(\rho, t)$ is the particle source and $\langle \rangle$ denotes flux surface averaging.

We utilise this equation in two ways to solve the underlying transport. In one case the Eq. (1) is solved inside a loop where non-linear optimisation algorithm is adjusting the transport coefficients D and v until best fit in χ^2 sense is found simultaneously for the modulated amplitude, phase and the steady state profiles. Time independent flux boundary condition is used at the outer boundary. Due to the uncertainty of the cold neutral source its magnitude (both the steady state and modulated part) are also fitted for best match while the shape of the profile is given by FRANTIC. The second way of using Eq. (1) is explained the next section.

3. D AND v FROM THE MEASURED AMPLITUDE AND PHASE PROFILES

For any periodic perturbation with time independent transport one can use the measured amplitude

and phase profiles of the perturbation to calculate the transport coefficients D and v [8]. In Ref. [8] these formulas were derived in a cylindrical plasma approximation. For completeness we write D and v starting from the more general geometry included in Eq. (1) while also retaining the source term. Using the same notation and the ansatz $n(\rho, t) = n_0(\rho) + A(\rho)\sin(\omega t - \varphi(\rho))$ together with $S(\rho, t) = S_0(\rho) + A_s(\rho)\sin(\omega t - \varphi_s(\rho))$ we arrive at similar equations:

$$D = -\omega \frac{Y \sin \varphi + X \cos \varphi}{A \varphi' V' \langle (\nabla \rho)^2 \rangle}, \quad v = -\omega \frac{(A' Y - \varphi' A X) \sin \varphi + (\varphi' A Y + A' X) \cos \varphi}{A^2 \varphi' V' \langle (\nabla \rho)^2 \rangle} \quad (2)$$

$$X = \int V' \left(A \cos \varphi + \frac{A_s}{\omega} \sin \varphi_s \right) d\rho, \quad Y = \int V' \left(A \sin \varphi - \frac{A_s}{\omega} \cos \varphi_s \right) d\rho$$

Figure 2 summarises the D and v profiles for the H-mode data set (#85228 – #85232) where GIM 4 was used using Equations (2) while neglecting any modulated source terms (valid inside 0.8). It is seen that in cases where the same modulation frequency was used the same amplitude profile is obtained with good accuracy. Another clear observation is that the measured amplitude increases with decreasing frequency as expected. Furthermore, the derived convective velocity is outwards (bottom frame). This is not compatible with the peaked steady state profile that in fact requires inward convection given the relatively small central fuelling from NBI.

It is possible to achieve a relatively good fit which simultaneously reproduces the observed steady state electron density but this requires sacrificing the perfect match in amplitude and phase. This is shown in Figure 3 where the iterative approach for solving D and v profiles is used. Clearly, the rapidly decaying amplitude and the flat phase are not matched exactly without outward convection. The same conclusion was obtained also in ASTRA transport code simulations. Some potential explanations for this are given below.

4. ELMS AND SAWTEETH

These discharges have both sawteeth ($\sim 4\text{Hz}$) and ELMs ($\sim 50\text{Hz}$) on top of the gas modulation induced transients. The effect of the gas puff modulation is completely masked by the sawteeth when their frequencies match too closely. In practise all of the 4Hz gas modulation phases in H-mode were found unusable. During an ELM particle transport increases significantly and cannot be considered to be time independent like we assume when solving transport from Eq. (1).

However, since within each modulation cycle several ELMs occur the transport we are solving is ELM-averaged transport which is time independent by definition. The remaining caveat is that ELM frequency itself is somewhat modulated by the gas puff modulation. Present analysis neglects this effect which could potentially change the transport at the gas modulation frequency.

5. THE COMPLEX PARTICLE SOURCE

The difficulties in simultaneously fitting the steady state and the perturbed amplitude and phase profiles may also be originating from too simplistic cold neutral source terms used in the modelling. Figure 5 shows tomographic inversion [9] of KL11 [10] data ($D\alpha$ video at 60Hz) on poloidal plane

for Pulse No: 85231 which feature both GIM 4 and GIM 8 modulation phases. Inversion has been done in the Minerva framework [11]. Note that the divertor GIM 12 was constantly on. In frame *b* the modulated emission reveals three distinct regions in the divertor area that contribute to the total modulated source: 1) direct source aligned with LFS separatrix, 2) recycling source on the inner divertor apron and 3) a volume source just left from the X-point. Of course one must keep in mind that the data is $D\alpha$ light and that proper interpretation requires SOL modelling. One can also see that modulations occur at different delays (frame *d*): The LFS radiation comes first and the HFS emission lags some 40 ms behind. Interestingly the volume emission is in anti-phase with the LFS emission. The frames *c* and *f* show the differences between GIM 4 and 8 confirming the expected trends. These data have not yet been fully utilised in SOL modelling but will provide valuable information for future work trying to clarify the particle sources. Further evidence for the need of better source understanding is shown in Figure 4 where an improved match was obtained in an exploratory ASTRA simulation that used warm neutrals (250eV) in addition to the 2eV cold neutrals.

6. L-MODE COLLISIONALITY SCAN

The gas modulation technique described above was also utilised in JET L-mode plasmas. These, yet unreported, discharges form a dimensionless 3-point collisionality scan which was achieved by changing temperature through NBI while keeping the density constant. As seen in Figure 6, the calculated profiles are roughly equal inside 0.6 where the modulated particle source is expected to be very small. This is consistent with the earlier experimental database study on JET [7] where in L-mode no collisionality dependence in density peaking was found. The result was also confirmed by a gyrokinetic quasi-linear analysis using QuaLiKiz [14] that found no trends within the scan. However, it is noted that weak collisionality dependence in the relevant L-mode parameter range was found with QuaLiKiz when using artificial parameters nulling the small but unavoidable T_e/T_i changes in the experimental scan.

DISCUSSION AND CONCLUSION

JET L-mode gas modulation experiments have shown that collisionality is not strongly affecting the particle transport, consistent with earlier experiments. The H-mode discharges in JET utilising this technique have shown that perturbation due to the modulated gas puff is reproducible with good accuracy thereby suggesting that the scheme has potential for future JET studies of H-mode particle transport e.g. by scanning q and collisionality. It was seen that gas modulation frequency must not coincide with sawtooth frequency in order to obtain reliable data. The measured electron density and the propagation of the density wave due to the gas puff have so far not been exhaustively explained. Several possibilities for resolution exist and include at least the NBI particle source modulation due to the density modulation, transport modification due to ELM frequency modulation and the additional complexities of the cold neutral source suggested by the $D\alpha$ camera data (see Figure 5). The inclusion of these factors is left for future work.

ACKNOWLEDGEMENTS

This work was supported by EURATOM and carried out within the framework of the European Fusion Development Agreement. The views and opinions expressed herein do not necessarily reflect those of the European Commission.

REFERENCES

- [1]. K.W. Gentle et al 1992 Nuclear Fusion **32** 217
- [2]. J O'Rourke et al 1993 Plasma Physics and Controlled Fusion **35** 585
- [3]. K. Nagashima et al 1993 Nuclear Fusion **33** 1677
- [4]. D.R. Baker et al 1998 Nuclear Fusion **38** 485
- [5]. E. Doyle et al 2012 Proceedings of IAEA FEC
- [6]. A. Sirinelli et al 2010 Review of Scientific Instruments **81** 10D939
- [7]. H. Weisen et al 2005 Nuclear Fusion **45**
- [8]. H Takenaga et al 1998 Plasma Physics and Controlled Fusion **40** 183
- [9]. J. Svensson 2011 EFDA–JET–PR(11)24
- [10]. A. Huber et al 2012 Review of Scientific Instruments **83**
- [11]. J. Svensson et al 2007 Proceedings of IEEE WISP
- [12]. R. Pasqualotto et al 2004 Review of Scientific Instruments **75**
- [13]. C.D. Challis et al 1989 Nuclear Fusion **29** 563
- [14]. C. Bourdelle et al 2007 Physics of Plasmas **14**, 112501

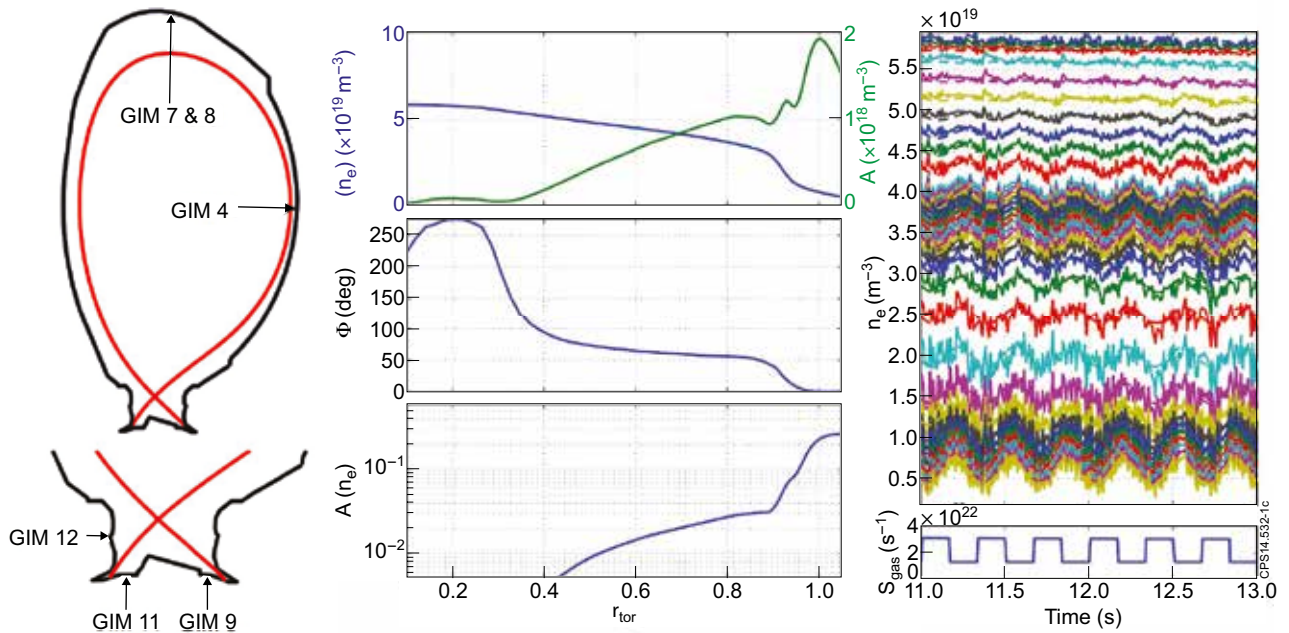


Figure 1: (left) Approximate gas injection locations in poloidal plane (middle) electron density profile and the modulation amplitude and phase profiles at 3Hz for Pulse No: 85231 (right) gas modulation waveform and the temporal density traces from reflectometer.

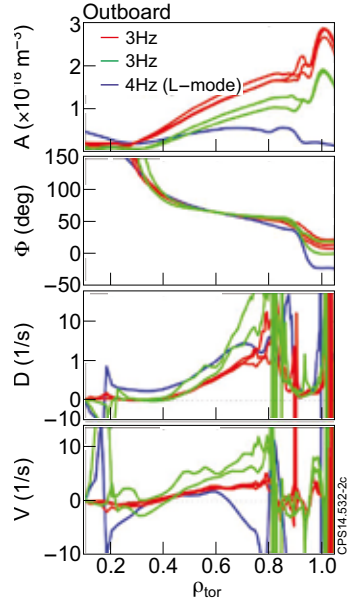


Figure 2: (top rows) Amplitude and phase profiles and (bottom rows) the D and V profiles of the GIM 4 data set.

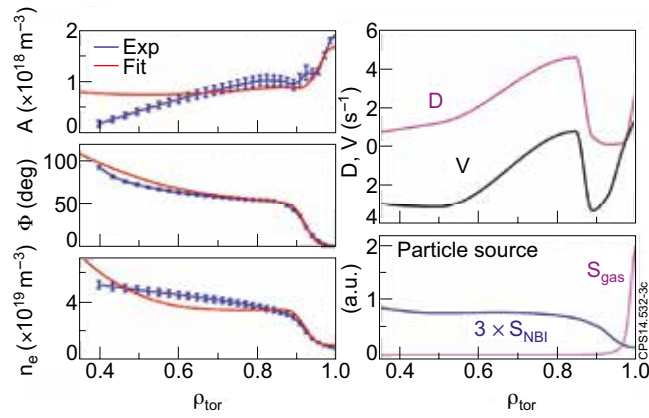


Figure 3: (left) Experimental and best fitting amplitude, phase and steady state for Pulse No: 85231 with GIM 4 modulation (right) the transport and source profiles.

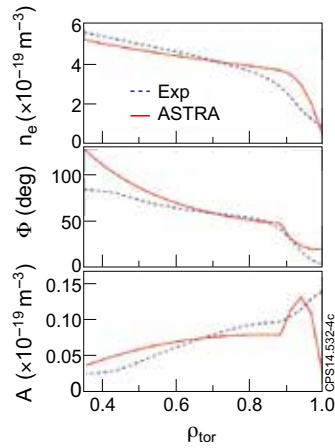


Figure 4: ASTRA fit with warm neutral contribution.

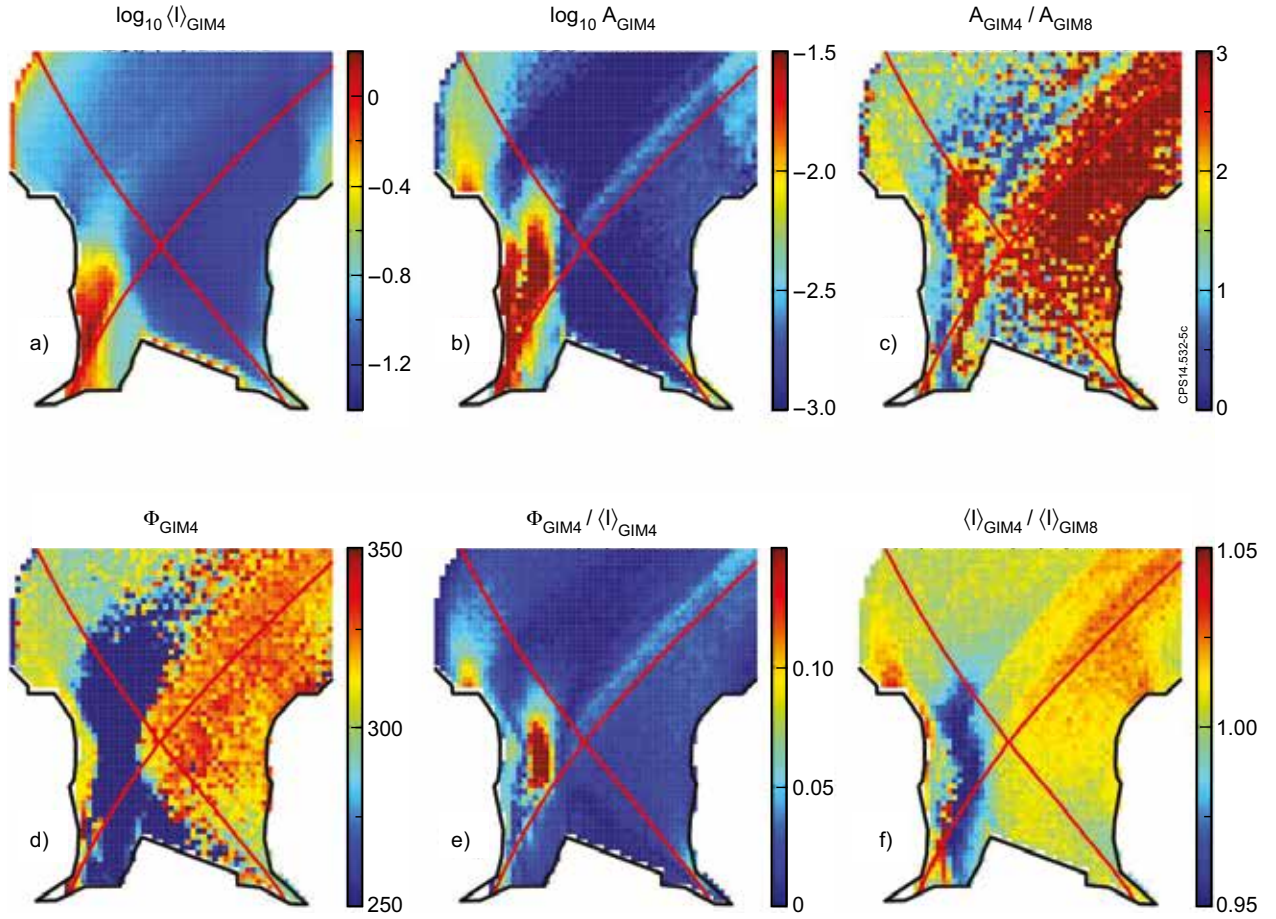


Figure 5: *Da* image data tomographically inverted [9] onto poloidal plane. a) time averaged intensity on log scale, b) 3Hz modulation amplitude on log scale, c) 3Hz amplitude ratio between GIMs 4 and 8, d) 3Hz modulation phase, e) ratio between the 3Hz modulation and steady state *Da* intensity, and f) *Da* ratio between GIMs 4 and 8.

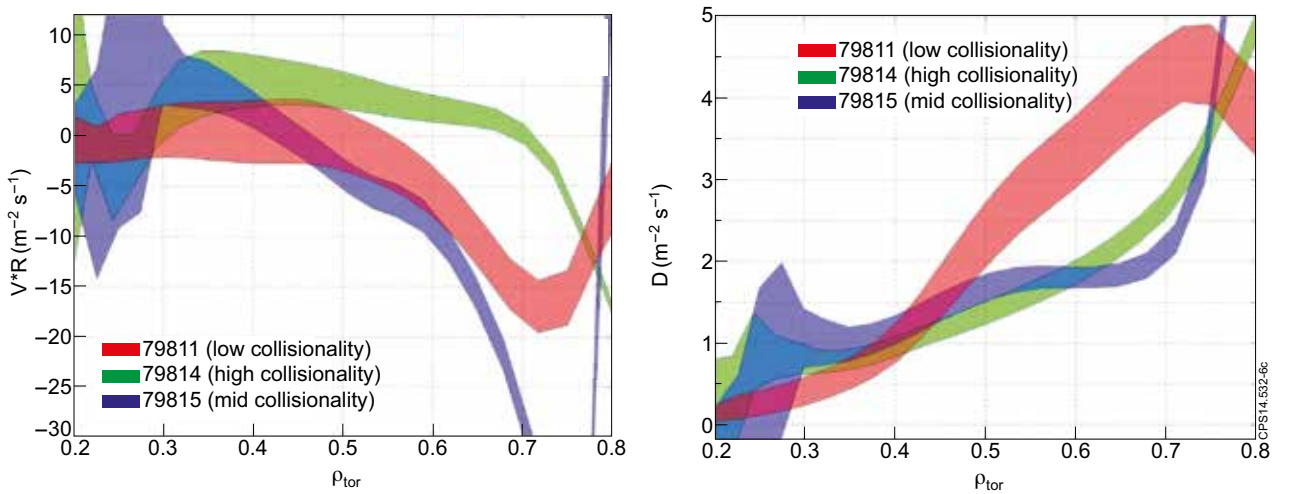


Figure 6: Derived *D* and *V* profiles for the L-mode collisionality scan. Note that the error estimate only takes into account the fluctuations in amplitude and phase profiles that depend on the choice of the time window.